A STUDY ON SOME TYPES OF SOLAR ENERGY

محمد علي عمار عون
المعهد العالي للعلوم والتقنية تاجوراء

المختار عبدالسلام امحمد دخيل
المعهد العالي للعلوم والتقنية ترهونة

الملخص

الغرض الأساسي من هذه الدراسة هو تطوير نظام مستدام لتحلية المياه بالتقطير الغشائي (SMDD) ترتبط وحدة التقطير بغشاء التلامس المباشر(DCMD) مباشر ببركة الطاقة الشمسية ذات التدرج الملوحة (SGSP) يحتوي النظام المستخدم على 0.1047 م من وحدة غشاء (PTFE) الكارهة للماء وانبوب تبريد يمتد على سطح مياه البركة يستخدم هذا النظام الماء الساخن وعالي الملوحة المستخرج من قطعة غير ملامسة (NCZ) كمحلول تغذية ثم يتم تصريف المحلول الملحي في منطقة الحمل السفلي (LCZ) للبركة الشمسية لذلك.

ومن الممكن استخدام المحلول الملحي المشبع لإنتاج الأملاح ، فلن يتبقى اي محلول ملحي مما يؤدي الى انخفاض تحلية المياه علاوةً على ذلك يتم استخدام انبوب نظام التبريد الخاص بالمياه المتخللة كنظام لأخماد الأمواج والتي تطفو فوق سطح مياه البركة.

تنتج هذه الموجات عن تيارات الرياح التي تكون مسؤولة عن اختلاط سطح البركة بشكل غير مرغوب فيه، ويتم تحليل النتائج وتقييم اداء النظام وسيتم عرضها في هذه الدراسة.

Abstract

The main purpose of this study is to develop a sustainable membrane distillation desalination (SMDD) system. Direct contact membrane distillation (DCMD) unit is connected directly to salinity gradient solar pond (SGSP). The used system contains 0.1047 m^2 of hydrophobic hydroporos PTFE membrane module and a cooling pipe running all over the pond water surface. This system uses hot and high concentrated saline water that is extracted from non-convictive zone (NCZ) as a feed solution. Then, the brine discharges at the lower convictive zone (LCZ) of

the solar pond. Therefore, if the saturated brine can be used to produce salts, there will not be any brine left over which may lead to low liquid discharge desalination. Furthermore, the cooling system pipe of permeate water is used as a wave suppression system where it is floating over the pond water surface. These waves are caused by wind driven currents which is responsible for undesirable pond surface mixing. The results are analysed and the system performance is being evaluated and will be presented in this project.

Key wards: zero liquid discharge desalination, membrane distillation, solar desalination, and solar pond.

Introduction

Since the beginning of life on the earth, the amount of fresh water remained almost the same while the population is in a rapid growing. This has put a huge stress on the available fresh water sources. Also, the severity of the water crisis has indirect effect which is water might not be sufficient for increased food demand. For instant, the United Nations has concluded that the major constraint to increase food production is not the lack of agriculture land, but it will be the water scarcity over the next few decades. Only 3% of available water is fresh water that can be accessed and easily utilized to become potable water which is obviously insufficient considering the rate of its consumption in basis of daily life. Also, 59% of saline water comes from seawater and 22% from brackish ground water sources, and the remaining from surface water and saline waste water. Recently, nearly 20% of the population is potentially in a need for fresh water, for this reason desalination of saline water is considered to be the practical solution for this crisis.

In fact, many desalination technologies have been developed over last few decades on the basis of thermal phase change, membrane separation, freezing, electro-dialysis, etc. But, the main technologies are based on the thermal and membrane processes. The thermal desalination usually includes phase changing; this technique contains different methods such as multistage flash MSF. The second method is the membrane desalination which includes reverse osmosis (RO), electro-dialysis (ED), and membrane distillation (MD). In RO process, fresh water under high pressure passes through semi-permeable membranes. The other type of membrane desalination is done by the difference in electric potential.

In this process, the salt ions are transported through ion-exchange membranes to another solution. It has been known that MSF, MED and RO will be dominant and competitive in the future. Recently, the total global desalination capacity has reached an 81 million m^3/day. It is predicted to produce over a 100 million m^3/day by 2015. Furthermore, for a global scale, 68% of the desalinated water is produced by membrane technology processes and 30% by thermal technology processes. However, there has been a dramatic increase in RO seawater desalination market basically due to its lower cost and simplicity. The third process is the MD, which is a thermally separation process resulted by a liquid phase changes.

Methodology

. Experiment and procedures:

The experiments were performed using a PTFE membrane manufactured by Membrane Solution (80 % porosity, 210 µm thickness, 0.22 µm nominal pore size). As it can be seen from

figure (3 a,b), the 0.1074 m^2 (0.235m W* 0.475 m L) flat membrane module has inlet and out let permeate and hot saline water. Both are flowing in counter directions and figure (3a, 3b) shows the used setup and the schematic diagram of the experiment.

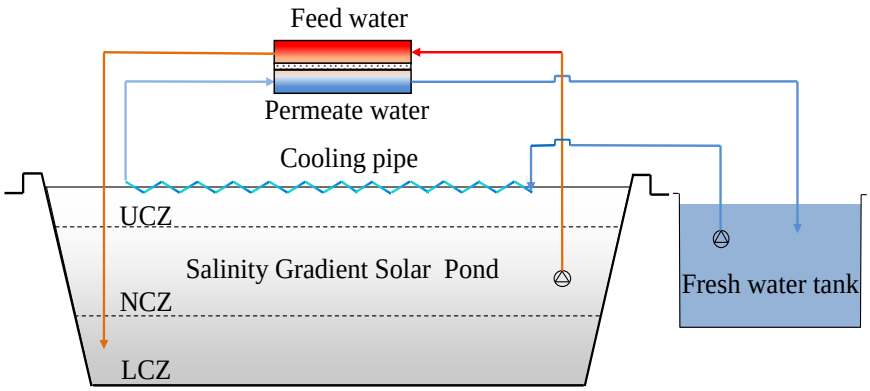

Fig. (1) the schematic diagram of experimental set-up

To conduct the distillation process, high concentrated (16 %) saline water is pumped from the NCZ layer of the SGSP at high temperature and inters the DCMD module after passing through water filter unit. The permeate water at cold side of the membrane is pumped from the distillate tank to the MD module at then circulating in a long pipe on the pond surface. This pipe is working as a cooling system to remove the heat gained by the permeate water through the distillation process. Also, it is used as wave suppressor to reduce the effect of wind on the SGSP water surface. Furthermore, temperature measurements are made at inlet and outlet of the MD module and 3 different thermocouples used through the set-up. In order to ensure that there is no penetration of the feed solution through the membrane, the conductivity of the permeate water is periodically measured. Finally, the discharged

saline water is injected at the LCZ of the SGSP. The temperatures of the bulk liquid phases are measured at the hot entrance (T_{f1}), the cold entrance (T_{p1}), the hot exit (T_{f2}) and the cold exit (T_{p2}), of the membrane module. These temperatures will be different from the temperatures at the hot and cold membrane surfaces T_{mf} and T_{mp}, respectively

Materials

Researchers studied many MD modules and factors affecting MD distilled water production associated with some applications of enhancement techniques. It has been applied for water desalination, a chemical solution treatment, environmental waste clean-up, water reuse and food processing. Moreover, it has been used for separation of zeotropic aqueous mixtures such as alcohol–water mixtures, concentration of radioactive solutions and application for nuclear desalination. It can be used for treatment of humic acid solutions, pharmaceutical waste water and in areas where high-temperature applications lead to degradation of process fluids.

Different membrane distillation configurations have been studied. The membrane configuration is defined as to the method of recovering the vapour after it has immigrated through membrane pores. The oldest membrane configuration is the direct contact membrane distillation (DCMD) where liquid phases are in direct contact with both surfaces of the membrane as shown in figure ( ). The other methods are air gap membrane distillation (AGMD), vacuum membrane distillation (VMD) and sweeping gas membrane distillation (SGMD) [10].

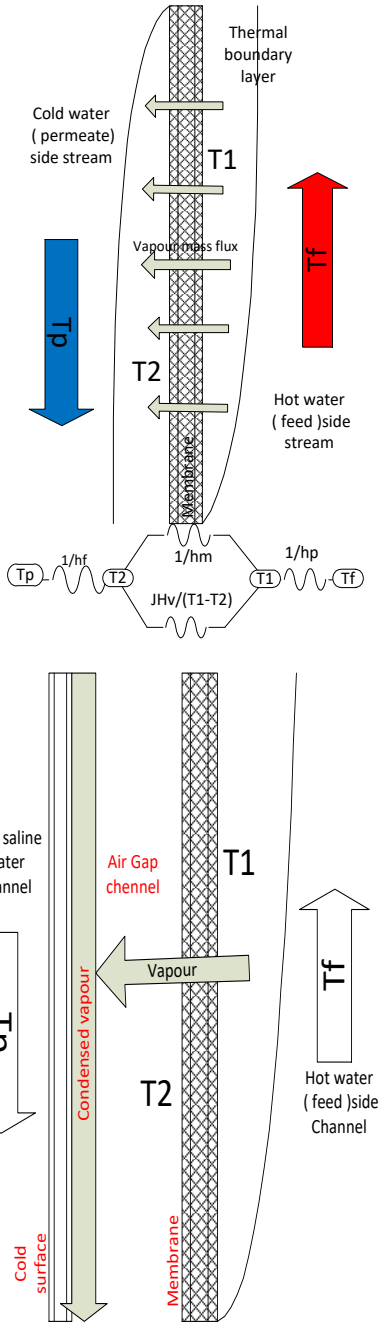

Fig.2. DCMD and AGMD configuration sketch and thermal layers

It should be known that DCMD is the most known desalination application as nearly 99 % rejection of non-volatile molecules solutions is usually achieved.

Fig.1. DCMD and AGMD configuration sketch and thermal layers

It should be known that DCMD is the most known desalination application as nearly 99 % rejection of non-volatile molecules solutions is usually achieved.

Moreover, normal desalination processes have a very high concentrated disposal with salinity of 70,000 PPM . Such rejection is a serious threat to the environment. It is expected that the installed capacity of water desalination plants and its brine discharge and energy consumption will increase to a significant level. This will cause a serious damage associated with the ecosystems. According to previous studies thermal desalination consumes approximately 1.3 KWh electricity and 48.5 KWh heat per each m3of desalinated water . Therefore, environmental friendly solution should be investigated to reduce the energy consumption and the brine discharge which eventually lead to reduce the carbon footprint and its environment effects.

2. Salinity-gradient solar pond (SGSP):

Salinity gradient solar ponds are large pool of salt water that has the ability of collecting and storing heat energy. Such a system is low in terms of cost and simple to design. This system can be used as a source of heat in different applications such as agriculture for aquaculture of fish breeding in winter. Also, it can be used for electricity power generation. Furthermore, solar ponds can be a great source of heat for desalination processes .A typical solar pond has three distinct zones. The top zone is called the Upper

Convective Zone (UCZ). It is located on the top of the solar pond and is the responsible zone of absorbing and transmitting the solar energy. In this zone the density is uniform and nearly equal to fresh water density. Then, the Non Convective Zone (NCZ), in this layer the saline water density increases linearly along the depth until the next layer. It acts as suppressor to avoid any heat loss; the convection currents are supressed as a result of the increase in the salinity. Also the temperature in this region gradually increases with the depth. The third zone called the Lower Convective Zone (LCZ) or storage zone. It is characterized of having uniform high temperature and density. As study has shown up to 40 % of the total received solar energy can be collected. Furthermore, temperatures up to 80°C can be reached in this region. A typical solar pond, density and temperature profile .

3. MD theoretical approach:

In MD, the driving force for water vapour transfer through the membrane pores is the temperature difference between the feed/membrane interface temperature (T_mf) and the permeate/membrane interface temperature (T_mp). This generates a vapour pressure difference between both membrane sides which forces the vapour molecules to travel through the membrane pores and condensate at cold membrane side.

3.1 Flow Mechanisms:

There are three basic mechanisms of mass flow inside the membrane wall, which are Knudsen diffusion, Poiseuille flow and molecular diffusion. In Knudsen diffusion, the pore size is too small, and the collision between molecules can be neglected. Furthermore, the collision between sphere molecules and the internal walls of the membrane is the dominant mass transport

form. Molecular diffusion occurs if the pore size is big comparing to the mean free path of molecules and they move corresponding to each other. The flow is considered Poiseuille (viscous flow) if the molecules act as continuous fluid inside the membrane pores. In general, different mechanisms occur simultaneously (Knudsen, Poiseuille and Molecular diffusion) inside the membrane if the pore size is less than 0.5 µm.

3.2 Knudsen number:

It is a governing quantity of the flow mechanism inside the membrane pores which is the ratio between the mean free path of the transported molecules and the pore size of the membrane. It is as follow:

$$kn=S/d \quad \ldots\ldots\ldots \quad (1)$$

S is the mean free path of the transferred gas molecule and d is the mean pore diameter of the membrane.

S is calculated from:

$$S=(k_B \quad T)/(\sqrt{2} \quad \pi P d_e^2 \quad) \quad \ldots\ldots\ldots \quad (2)$$

The pore sizes of the most membranes are in the range of 0.2 -1.0 µm. The mean free path of water vapour is 0.11 µm at feed temperature of 60°c. Therefor kn is the range of 0.11-0.55 [20].

The different flow mechanisms inside the membrane pores can be identified by Knudsen number (kn):

kn <0.01 Molecular diffusion

0.01<kn<1 Knudsen-molecular diffusion transition mechanism

kn>1 Knudsen mechanism

3.3 Mass Flux (J):

As shown in figure (2), vapour is transferred from feed side of the membrane to the permeate side by pressure difference force which is resulted from the temperature difference between two sides. The mass transfer may be written as a linear function of the vapour pressure difference across the membrane, given by:

J=C_m (P_1-P_2) kg/m^2/sec …….. (3)

Where J is the mass flux, C_m is the membrane distillation coefficient, and P_1,P_2 are the partial pressure of water vapour evaluated at the membrane surface temperatures T_1 ,T_2.

C_m for Knudsen flow mechanisms:

〖 C〗 _m^k=2εr/3τδ (8M/πRT)^(1⁄2) (4)

C_m for molecular diffusion

C_m^D=ε/τδ PD/P_a M/RT (5)

C_m for Knudsen-molecular diffusion transition mechanism:

C_m^C=[3/2 τδ/εd (πRT/8M)^(1⁄2)+τδ/ε Pa/PD RT/M]^(-1) (6)

D is the diffusion coefficient of the vapour in the air. P is the pressure at $\bar{T}$ and can be found using Antoine equation:

P^v=exp〖(23.238-3841/($\bar{T}$-45))〗 (7a)

($\bar{T}$) is the average membrane temperature.

The vapour pressure decreases with increasing of feed water salinity according to Raoult's law as follow [21]:

P_c^v=(1-x_c) P^v (7b)

Where xc is the weight fraction of salt in water.

3.4 Heat Flux (q):

The heat transfer models of MD can be summarized as follows:

Convective heat transfer from the feed side to the membrane surface boundary layer:

q_f=h_f (T_f-T_mf) (8)

Where qf is the feed heat flux (W/m2) and h_f is the heat transfer coefficient (W/m2.K).

Heat flux through the membrane which includes conduction heat flux through the solid material of the membrane k_m dt/dx , and the latent heat transfer as a conviction by water vapour through the pores JH_v:

q_m=JH_v+k_m dT/dx (9)

H_v is the vaporisation enthalpy of water evaluated at the mean temperature (T_mf+T_mp)/2 , and the second term is the conduction heat loss through the membrane material.

Finally, heat is transferred through the permeate boundary layer to the permeate water by convection.

q_p=h_p (T_mp-T_p) (10)

At steady state:

q_f=q_m=q_p (11)

The overall heat transfer coefficient can be determined by:

U=[1/h_f +1/(k_m/δ_m +(JH_v)/(T_mf-T_mp))+1/h_p]^(-1) (12)

The rate of total heat transferred through the membrane is:

〖 q〗_t=U (T_(f)_ T_p) (13)

The feed flow energy balance is:

q_f=m ̇_(f) c_p (T_(f,in)-T_(f,out)) (14)

The thermal efficiency of the MD system is:

E_t (%)= (JH_v A)/Q_t *100 (15)

The thermal efficiency is the ratio between the water thermal energy consumption to generate vapour and the total energy supplied to the system. Whereas, heat conduction through solid portion of membrane is considered as heat loss and it should be minimised to improve the thermal efficiency.

To be more accurate, the efficiency should include both thermal and electrical energy flow rate (pumps) thus GOR (Gained Output Ratio) can define it as:

GOR=(JH_v A)/(E ̇_T+E ̇_E) (16)

To determine heat transfer coefficients of the boundary layers at both membrane sides the average bulk temperature of feed side (T_f+T_mf)/2 , and at permeate side (T_mp+T_p)/2 of the membrane should be used. Graetz-Leveque recommends [22]:

N_u=1.86 (R_e P_r d_h/L)^0.33 d_h=(4A_c)/P_e (17)

This correlation can be used for laminar flow (Re < 2100).

In contrast, next correlation can be applied for turbulent flow(2500<R_e<1.25* 〖10〗^5 and 0.6<P_r<100).

N_u=0.023 〖Re〗^0.8 〖Pr〗^n (18)

Where n is equal to 0.4 for heating, and 0.3 for cooling .

The dimensionless groups, Nusselt number (Nu), Reynolds number (Re) and Prandtl number (P_r) can be calculated using the available physical data of feed and permeate fluid.

At both sides of the membrane where the vapour-liquid interface takes place; there is a thermal boundary layer with temperature different from the bulk stream. This difference is described by temperature polarisation coefficient (TPC).

TPC=(T_mf-T_mp)/(T_f-T_p) (19)

Analytical model is an iterative method to predict T_mf and T_mp. Then by entering the geometry and fluid properties in the model, the boundary heat transfer coefficients are calculated and they can be used. Then it uses the values of T_mf and T_(mp) which are initially assumed equal to the bulk temperature T_f and T_p respectively, to determine the new values of T_mf and T_mp by

a number of iterations. Equations (21) and (22) are used to predict both temperatures. Once the surface temperatures T_mf and T_(mp) are determined, the software calculates the rest of required parameters. See appendix (A).

To determine the evaporation latent heat:

H_v is evaluated at T

$$T=(T_{mf}+T_{mp})/2 \quad (20)$$

From heat balance through the membrane and boundary layers:

Tmf=(h_m (Tp+(h_f⁄h_p) Tf)+hf Tf-JH_v)/(h_m+h_f (1+h_m⁄h_p)) (21)

Tmp=(hm (Tf+(hp⁄h_f) Tp)+hp Tp+JHv)/(hm+hp (1+h_m⁄h_f)) (22)

hm=km/δ_m …….. (23)

4. Fresh water production:

DCMD operational parameters are selected (e.g., membrane type, feed and permeate velocity, partial pressure of air entrapped in the pores) and the SGSP specifications (e.g., surface area, thickness of each zone) are determined, the performance of SZLDD system is evaluated. Moreover, saline water and heat extracted from the SGSP, mass flux and energy required for permeate water production through the membrane are determined. The necessary membrane surface area to use all the energy collected in the SGSP is also determined. In addition, the required membrane area ADCMD (m2) for the DCMD module, when the brine extracted from the SGSP is used without losses, can be found by equating the energy stored in the SGSP with the energy consumed by the DCMD module. Thus:

(A〗_SP*q_useful)*e_sp=A_DCMD*qm (29)

ASP (m2) is the surface area of the SGSP.

The water flow produced by DCMD module, qm (m3/s), is given by:

$$qm = (J*A\_DCMD)/\rho \quad (30)$$

Fig (3) shows the DCMD module and the SGSP coupling. The feed solution to the membrane module is the hot saline water that is extracted from the lowest layer of NCZ of the solar pond. The concentration of supplied brine is about 16 % (160 g/l) at average of 45°C. It is transferred to the DCMD module through the feed channel then it is discharged in the LCZ layer through the pile salt charger. On the other side, the permeate water in circulated through the long cooling pipe that is located on the top of the solar pond surface. Actually, it is working as wave suppressor to prevent pond mixing. Also, since the permeate water gains some mass and heat after exiting the DCMD module, the cooling pipe maintain its temperature at lowest value then eventually keeping higher temperature difference.

The feed water is gradually heated from ambient to LCZ temperature which reduces irreversibility. It is assumed that there are no heat losses in the coupled system. Therefore, the average feed temperature is assumed to be equal to the temperature in the LCZ which is considered as Tsp, i.e., Tf inlet = Tsp = TL, where TL is the LCZ temperature. Also, a stainless steel cross flow heat exchanger (fig.3 HE1) is connected to the DCMD module and the evaporation pond to exchange heat between the outlet fresh water that is slightly hot and cold inlet feed water. In this way, the average permeate temperature is consistency kept stable at temperature ranging from 20°C to 23°C. Furthermore, for energy conservative purpose, second heat exchanger (HE2) is installed to

recover heat from the hot feed water exiting the MD module and preheat the feed water that inters the in-pond heat exchanger pipe in the solar pond.

5. SGSP heat extraction:

A salinity gradient solar pond of 50 m2 located at RMIT Bundoora east campus, Australia, in renewable energy laboratory is used to supply hot saline water to DCMD module. The RMIT solar pond is 2.05 m deep, and the bottom storage zone is 0.56 m thick. Also, the gradient zone is 1.34 m thick and the top convective zone is 0.15 m thick.

The rate of extracted thermal energy is given by:

$$Q = (mf) * Cp * (Tpo - Tpi) \quad (24)$$

Where m is the mass flow rate (in kg/s) and Cp (in J/kg °C) is the specific heat of the extracting hot saline water from the SGSP.

The solar pond efficiency can then be calculated by [24]:

$$〖e〗_{sp} = (m * 〖C〗_p * (Tpo - Tpi)) / (G * Asp) \quad (25)$$

Where G is the solar radiation at the surface of the pond (in W/m2) and Asp is the area of solar pond.

Results and Discussion:

In order to optimise the DCMD system, a mathematical module is used to predict the related parameters of the MD such as type and the thickness of the membrane sheet. Fig.5 shows the variation of the mass flux and energy consumption with the membrane active layer thickness. It can be seen that as the thickness increases, the mass flux decreases as well as the energy consumption. On the other hand, as the thickness decreased, they increase to a high value. As a result, the mass and thermal energy consumption is associated and they relay partially on the

membrane thickness. Therefore, the membrane thickness between 40 and 80 µm is selected to be used with the DCMD module.

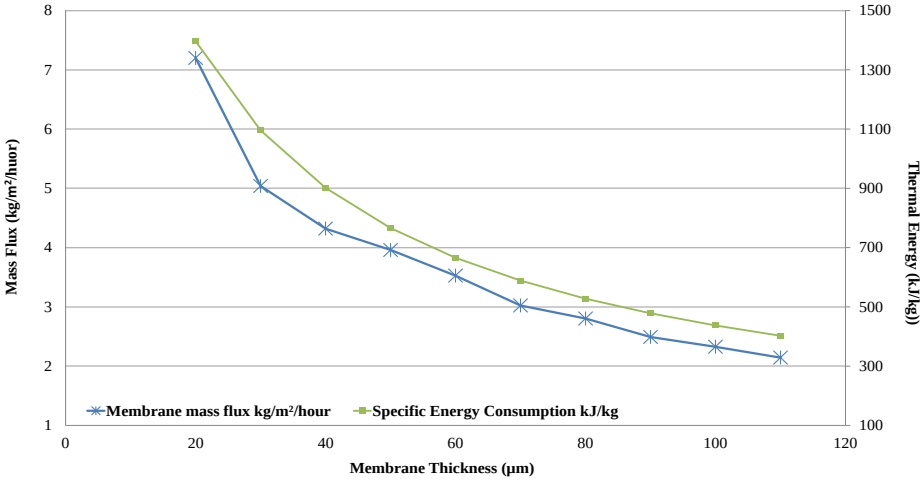

Fig(3) Heat and mass transfer variation with membrane thickness, the temperature difference is 20° and the mass flow at both sides is 5 l/min

7.1 MD performance:

Fig. 3. Shows an example of the variation of the temperature during the distillation process at different points in the set-up. These temperatures are used along with mathematical model to predict the permeate water mass flux, heat flux across the membrane and the thermal energy consumption. Also, they are used to evaluate the thermal performance of the sustainable membrane distillation system. The inlet feed temperature is about 49.5 °C and the average permeate temperature is about 26.5 °C.

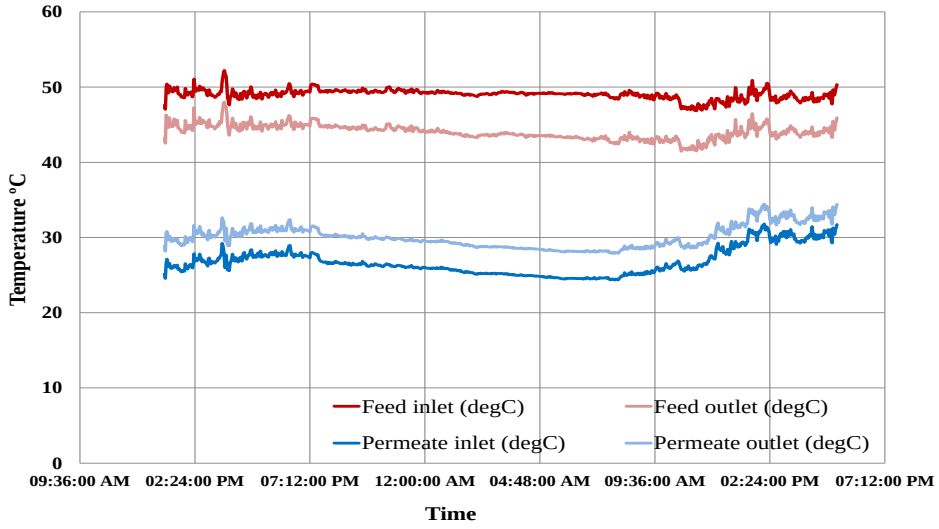

Fig (4). inlet and outlet temperatures at different locations of the Set-up with day and night time duration

Fig. 4 shows the predicted and experimental mass flux of permeate water at various feed water flow rates when the system is in study state condition. The experimental data corresponded well to the mass flux estimated by the Knudsen diffusion model and it increase from 1.4 kg/m²/hr to 2.2 kg/m²/hr. Accordingly, the trans-membrane coefficient is 0.001 kg/m²/Pa/hr. However, it can be seen that the experimental data is in reasonable agreement with the mathematical model limits since the estimated result is higher by 20 % in average. Hence, the Knudsen diffusion is the dominant mechanism in mass transfer across the membrane; it has been found that a Knudsen number value is about 8.8.

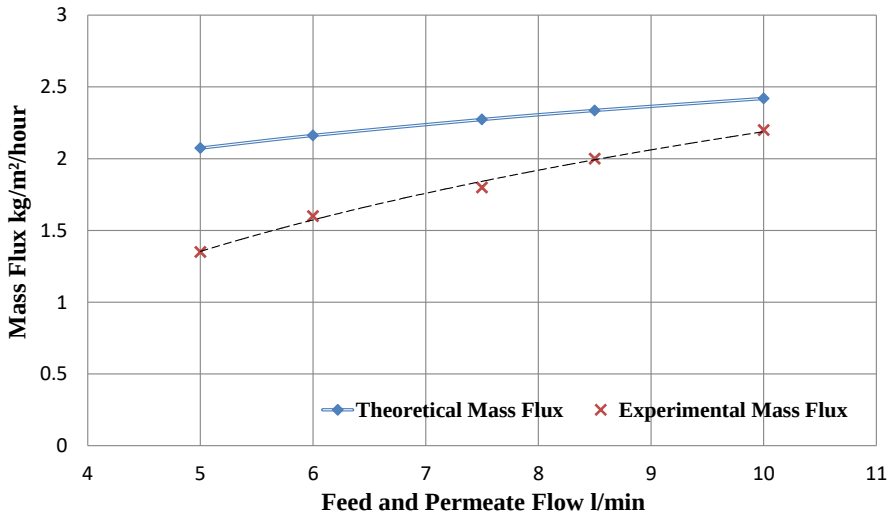

Fig(5) . Membrane mass flux (J) across the membrane variation with feed and permeate mass flow rate

The tortuosity factor (τ) plays a vital role in determining the mass transport mechanism. In this work, the tortuosity of 1.5 is employed and it is derived from the correlation proposed by Khayet. Furthermore, TPCs ranged between 30% and 36% depending on feed water flow rate which is varying from 5 l/min to 10 l/min. This contributed to the large difference in temperature between the bulk feed stream and the membrane surface, and the pronounced effect of temperature polarization. The increase in heat transfer coefficient in boundary layer might be induced by the high cross flow velocity which will result in the decrease in temperature difference between bulk streams and membrane surfaces.

7.2 Energy consumption:

The membrane permeate mass flux considerably increases with the increase of the mass flow rates at both sides of the

membrane which result in an increase in thermal energy consumption.

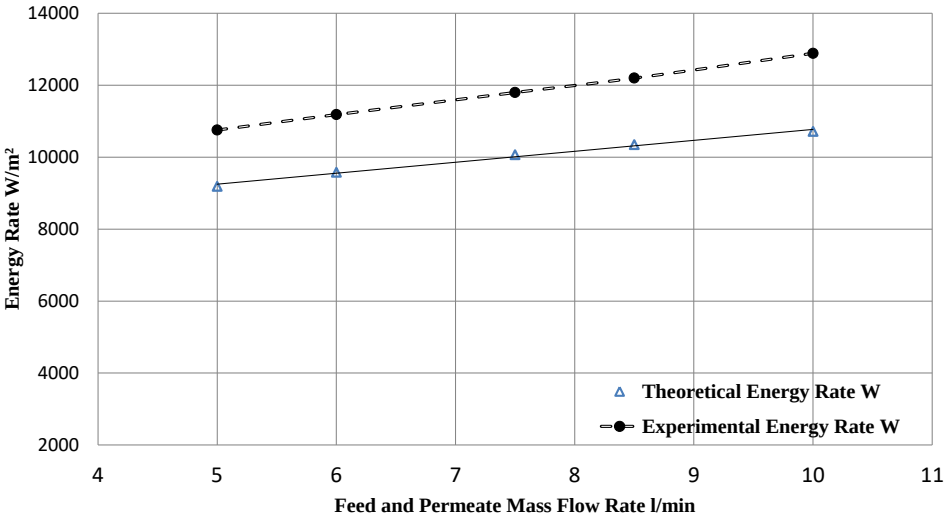

Fig.(6) . the energy consumption of this system varies with feed and permeate mass flow rate

The increase of the total thermal energy entering the channels, results in the decrease of the bulk temperature difference across the membrane. According to eqn. this effect leads to a higher driving force. Also, the temperature polarisation is reduced by an enhanced heat transfer in the thermal boundary layers, thus a higher interfacial temperature difference needs to be used. Fig (6) shows how the energy consumption rate of this system varies with mass flow rates theoretically and experimentally. It ranges from around 9000 W/m² to less than 11000 W/m². This energy rate consists of evaporation, conduction and lost thermal energy. It has been observed that the difference between the experimental and prediction value is at the average of 16% depends on the mass flow rate at both sides. The higher total energy demand is not

completely compensated by higher inlet temperatures from an energetic point of view. Also, the high thermal energy input and the heat transfer are not sufficient to raise the vapour driving force accordingly. Also, the pipe that is positioned on the top surface of the pond works perfectly and kept the output permeate water at exactly the temperature of the pond water surface. Also it is successful with keeping the pond water surface stable by breaking the waves that is caused by wind turbulent currents. A short video is provided to watch this pipe in action in this reference.

7.3 Water production by SGSP:

The coupled DCMD/SGSP through the NCZ and discharging brine water in the pond at LCZ layer and operating system with T_f = 29.5 ºC and T_p = 45 ºC, is shown in figure 3.

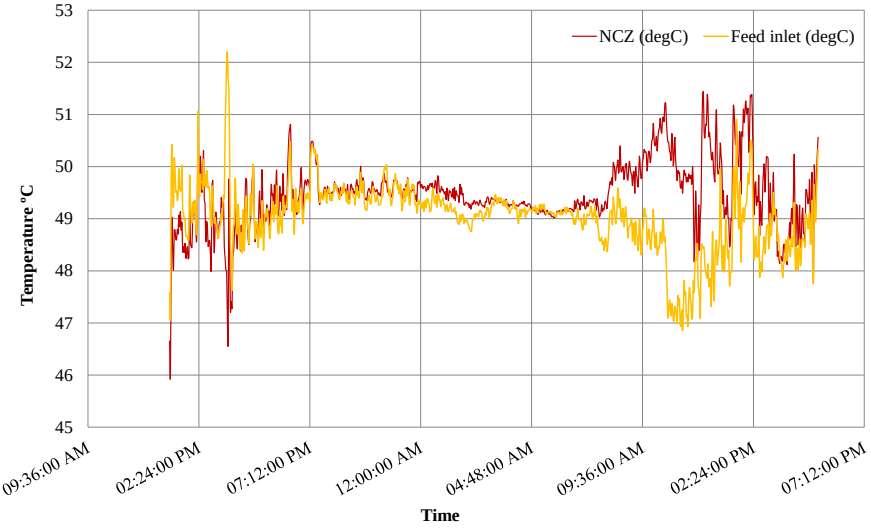

Fig(7). day and night temperature at NCZ and DCMD feed inlet temperature

The actual NCZ temperature which represents the SGSP temperature in presented along with inlet feed temperature in

figure (7) for comparison aspect. Furthermore, it can be noticed that the night performance of the experiment is not steady where the temperature of saline water slightly decreases. It may occur due to the effect of heat loss through the pond water surface and DCMD system components. On the day time, the feed inlet temperature to the DCMD approaches LCZ temperature which means the heat transfer and heat loss is very small. Moreover, during the winter season the LCZ temperature decreases gradually and this affects the feed water temperature. Eventually, the vapour pressure on the feed side and the permeate mass flux decrease. Thus, as shown in figure 5 and 7, the highest water mass flux obtained in the DCMD module occurs when the feed side is at 49.5°C and the mass flow rate is 10 l/min. At these conditions, when treating a feed solution with a salinity of 16 %, the coupled system delivers 52 l/day of fresh water per m^2 of membrane or l/day per m^2 of membrane and m^2 of SGSP. If LCZ temperatures are higher, the coupled system will produce larger water permeate flux. However, lower temperature in the LCZ would decrease the temperature of the feed saline water flowing to the DCMD module. It is also worthy to mention that this system almost terminates the liquid discharge by using the brine to feed the LCZ of SGSP. It is delivered at slightly less temperature but at higher density. In certain cases with saturated concentration brine, it can be used to feed an evaporation pond to produce row salts.

Conclusion

Direct contact membrane distillation (DCMD) unit has been connected directly to salinity gradient solar pond (SGSP) through to achieve sustainability. The feed brine of DCMD is 16% concentrated water at 49.5 ºC with different mass flow rates at both

sides of the membrane. The mass flux model prediction is at an 80% agreement with the experimental data value.

In agreement with different studies, the trans-membrane coefficient of the used PTFE membrane is proved to be 0.001 kg/ m2/Pa/ hour. Also, the system can deliver 52 l/day of fresh water for m2 of membrane coupled with SGSP consuming around 11 kW/ m2 as an instant thermal energy.

Furthermore, the cooling system pipe of the permeate water is used as suppression system on the top of the SGSP water surface and from the observation it works and successfully stabilizes the water surface under rough conditions.

Finally, this study is an essential work to understand the performance of the direct coupled DCMD with SGSP which may lead to sustainable membrane distillation system. Further investigation is required to improve the system which may include an economic assessment study to determine the ability of this system to be introduced to the market.

References

1. McNicoll, G., *United Nations Development Programme: Human Development Report 2006. Beyond Scarcity: Power, Poverty and the Global Water Crisis.* Population and Development Review, 2007. **33**: p. 198+.
2. Ghaffour, N., et al., *Renewable energy-driven desalination technologies: A comprehensive review on challenges and potential applications of integrated systems.* Desalination, 2015. **356**(0): p. 94-114.
3. Nakoa, K., A. Date, and A. Akbarzadeh, *A research on water desalination using membrane distillation.* Desalination and Water Treatment, 2014: p. 1-13.

4. Karagiannis, I.C. and P.G. Soldatos, *Water desalination cost literature: review and assessment.* Desalination, 2008. **223**(1–3): p. 448-456.
5. Ghaffour, N., T.M. Missimer, and G.L. Amy, *Technical review and evaluation of the economics of water desalination: Current and future challenges for better water supply sustainability.* Desalination, 2013. **309**(0): p. 197-207.
6. Rodríguez, J.R.B., et al., *Distilled and drinkable water quality produced by solar membrane distillation technology*. Desalination and Water Treatment, 2012. **51**(4-6): p. 1265-1271.
7. Khayet, M., C. Cojocaru, and G. Zakrzewska-Trznadel, *Studies on pervaporation separation of acetone, acetonitrile and ethanol from aqueous solutions.* Separation and Purification Technology, 2008. **63**(2): p. 303-310.
8. Khayet, M., *Treatment of radioactive wastewater solutions by direct contact membrane distillation using surface modified membranes.* Desalination, 2013. **321**(0): p. 60-66.
9. Khayet, M., A. Velázquez, and J.I. Mengual, *Direct contact membrane distillation of humic acid solutions.* Journal of Membrane Science, 2004. **240**(1–2): p. 123-128.
10. Khayet, M., *Membranes and theoretical modeling of membrane distillation: A review.* Advances in Colloid and Interface Science, 2011. **164**(1–2): p. 56-88.
11. Kalogirou, S.A., *Seawater desalination using renewable energy sources.* Progress in Energy and Combustion Science, 2005. **31**(3): p. 242-281.
12. Sadhwani, J.J., J.M. Veza, and C. Santana, *Case studies on environmental impact of seawater desalination.* Desalination, 2005. **185**(1–3): p. 1-8.
13. Wetterau, G., *Desalination of Seawater*. Vol. 61. 2011: American Water Works Association.

14. Lattemann, S. and T. Höpner, *Environmental impact and impact assessment of seawater desalination.* Desalination, 2008. **220**(1–3): p. 1-15.
15. Mesa, A.A., C.M. Gómez, and R.U. Azpitarte, *Energy saving and desalination of water.* Desalination, 1997. **108**(1–3): p. 43-50.
16. Leblanc, J., et al., *Heat extraction methods from salinity-gradient solar ponds and introduction of a novel system of heat extraction for improved efficiency.* Solar Energy, 2011. **85**(12): p. 3103-3142.
17. Velmurugan, V. and K. Srithar, *Prospects and scopes of solar pond: A detailed review.* Renewable and Sustainable Energy Reviews, 2008. **12**(8): p. 2253-2263.
18. Hassairi, M., M.J. Safi, and S. Chibani, *Natural brine solar pond: an experimental study.* Solar Energy, 2001. **70**(1): p. 45-50.
19. Malik, N., et al., *Monitoring and maintaining the water clarity of salinity gradient solar ponds.* Solar Energy, 2011. **85**(11): p. 2987-2996.
20. Alkhudhiri, A., N. Darwish, and N. Hilal, *Membrane distillation: A comprehensive review.* Desalination, 2012. **287**(0): p. 2-18.
21. *Solar pond suppression pipe.* *https://www.youtube.com/watch?v=HVCGe3tTkYE&feature=youtu.be*.